Photosynthesis Research **39**: 39–50, 1994.

Regular paper

Range of photosynthetic control of postillumination $P700^+$ reduction rate in sunflower leaves

Agu Laisk & Vello Oja
Institute of Molecular and Cell Biology, Tartu University, Riia str. 181 Tartu, Estonia EE2400

Received: 11 May 1993; accepted in revised form 29 September 1993

Key words: Photosynthetic control, 830 nm absorbance, P700

Abstract

The kinetics of the postillumination reduction of $P700^+$ which reflects the rate constant for plastoquinol (PQH_2) oxidation was recorded in sunflower leaves at different photon absorption densities (PAD), CO_2 and O_2 concentrations. The P700 oxidation state was calculated from the leaf transmittance at 830 nm logged at 50 μs intervals. The $P700^+$ dark reduction kinetics were fitted with two exponents with time constants of 6.5 and about 45 ms at atmospheric CO_2 and O_2 concentrations. The time constant of the fast component, which is the major contributor to the linear electron transport rate (ETR), did not change over the range of PADs of 14.5 to 134 nmol cm^{-2} s^{-1} in 21% O_2, but it increased up to 40 ms under severe limitation of ETR at low O_2 and CO_2. The acceptor side of Photosystem I (PS I) became reduced in correlation with the downregulation of the PQH_2 oxidation rate constant. It is concluded that thylakoid pH-related downregulation of the PQH_2 oxidation rate constant (photosynthetic control) is not present under normal atmospheric conditions but appears under severe limitation of the availability of electron acceptors. The measured range of photosynthetic control fits with the maximum variation of ETR under natural stress in C_3 plants. Increasing the carboxylase/oxygenase specificity would lead to higher reduction of the PS I acceptor side under stress.

Abbreviations: Cyt b_6f – cytochrome b_6f complex; C_w – cell-wall CO_2 concentration, μM; ETR – electron transport rate; Fd – ferredoxin; FNR – ferredoxin-NADP reductase; FRL – far-red light; PC – plastocyanin; PAD – photon absorption density nmol cm^{-2} s^{-1}; PFD – photon flux density nmol cm^{-2} s^{-1}; PS I – Photosystem I complex; PQ – plastoquinon; PQH_2 – plastoquinol; PS II – Photosystem II complex; P700 – Photosystem I donor pigment, reduced; S830 – 830 nm signal (D830, difference of S830 from the dark level); WL – white light; Y_I – maximum quantum yield of PS I electron transport, rel. un.

Introduction

In photosynthesis, electrons are transported from PS II through a sequence of carriers, PQH_2, Cyt b_6f, PC, to P700. The slowest reaction in this sequence is PQH_2 oxidation which is coupled to proton transfer into the thylakoid lumen (Stiehl and Witt 1969, Bendall 1982, Rich 1982). In the presence of sufficient PQH_2, the rate of this reaction is controlled by intrathylakoid pH. This process is known as photosynthetic control (Siggel 1974, 1976, Bendall 1982, Foyer et al. 1990, Harbinson et al. 1990).

In isolated thylakoids and chloroplasts, rates are lower when electron transport is coupled to proton transfer and ATP synthesis, indicating the presence of the photosynthetic control. In intact leaves the actual electron transport rates are high, approaching the maximum (uncoupled)

electron transport rates in chloroplasts (Foyer et al. 1990). This raises a question, is the photosynthetic control normally present in leaves, or it is activated only when electron transport is severely restricted downstream from PS I (e.g., limited CO_2 supply)?

The question of the photosynthetic control of PQH_2 oxidation rate was addressed by Harbinson and Hedley (1989) who measured the speed of postillumination reduction of $P700^+$, using leaf absorbance changes around 820 nm. Under intense light a considerable fraction of the pigment stays oxidised as a result of balance between the limited supply from PQH_2 and rapid removal of electrons from P700 (Weis et al. 1987, Weis and Lechtenberg 1989). After a sudden darkening, oxidation of PQH_2 continues. The transfer of electrons through the immediate precursors of P700, Cyt *f* and PC occurs in the time-range far below 1 ms (Haehnel 1982, 1984, Haehnel et al. 1980), so that these compounds are in near-equilibrium redox relationships with P700 even during fast photosynthetic electron transport (Joliot and Joliot 1984, Harbinson and Hedley 1989).

It is expected that in the presence of photosynthetic control the time constant for postillumination $P700^+$ reduction increases. When light was switched on after a long dark exposure, the $t_{1/2}$ of $P700^+$ reduction decreased from 10 to 5 ms during photosynthetic induction in pea leaves (Harbinson and Hedley 1989) but, contrary to expectations, the $t_{1/2}$ did not change over a range of light intensities from 400 to 1400 $\mu mol\, m^{-2}\, s^{-1}$. A slight increase of the half-reduction time was recorded under 2% O_2 (Genty et al. 1990). Evidently, the conditions and maximum range of functioning the photosynthetic control in intact leaves needs to be further studied.

In this work we measure postillumination $P700^+$ reduction kinetics under a variety of conditions of irradiance and CO_2 concentration in sunflower leaves. The leaf absorbance around 830 nm has been used as a signal reflecting P700 oxidation state (Weis et al. 1987, Harbinson and Woodward 1987, Harbinson et al. 1989, Weis and Lechtenberg 1989, Foyer et al. 1990, Harbinson et al. 1990, Genty et al. 1990, Lechtenberg et al. 1990). We confirm the results of Harbinson and Hedley (1989) and extend their studies showing the extent of the photosynthetic control and its relation to the acceptor side reduction of PS I.

Material and methods

Sunflower (*Helianthus annuus* L.) plants were grown in a growth chamber at PFD of 46 $nmol\, cm^{-2}\, s^{-1}$, 18/6 h day/night cycle, air temperature 25/15 °C day/night, R.H. 50 to 60% by day, on well-fertilized peat-soil mixture. Attached upper fully expanded leaves of 4-week-old plants were used in measurements.

The gas exchange apparatus contains an open gas flow system in which the gas composition can be adjusted (Oja 1983). CO_2 and water vapour (analyser LI-6262, LiCor, Lincoln, Nebraska) and O_2 (analyser Ametek S-3A, Process and Analytical Instruments Division, Pittsburgh, PA) exchange rates are measured. During the measurements the leaf is enclosed in a sandwich-type cuvette ($4.4 \times 4.4 \times 0.3\, cm^3$, gas flow rate $20\, cm^3\, s^{-1}$). For temperature stabilization the leaf blade is fixed with starch paste directly to the cuvette window, thermostated by water from the other side. This also avoids leaf movements and reduces the noise of the 830 nm signal. Gas exchange proceeds via the lower epidermis of the leaf only, but this is accounted for, calculating the cell-wall CO_2 concentration (C_w) on the basis of diffusion resistances and the solubility of CO_2 (Laisk 1977). The system response-times, determined mainly by gas flow/volume ratios, are 0.5 s for O_2 and 2.5 s for CO_2. The CO_2 and O_2 monitors are calibrated by means of dynamic capillary gas mixers which allow one to adjust CO_2 and O_2 concentrations with better than 1% accuracy in the range from 0 to 2000 ppm (Oja 1983).

A special six branch fiber-optic has been designed for leaf illumination and optical measurements. Plastic fibers of 1 mm diameter (Toray polymer optical fiber, PF-series, from Laser Components, Gröbenzell/Mü, Germany) are arranged into a bundle of $45 \times 45\, mm^2$ which is attached to the leaf cuvette. The free ends of the fibers are divided into six branches from which three are used for illumination and three

for gathering optical signals from the leaf. The fibers coming from the three light sources are equally spaced over the leaf area. Some fibres of each illumination bundle are directed to a LI-190SB and arranged so that the quantum sensor shows the PFD in the centre of the chamber while leaf is enclosed. The light profile over the leaf area was studied and found to be close to the Gaussian distribution with half-width ± 15%. Corrections relating PFD in the centre to mean and to PFD at the site of 830 nm measurement are taken into account.

The 830 nm signal is measured in the transmission mode (Schreiber et al. 1988) in a spot of 10 mm diameter placed excentrically in the leaf chamber in order to avoid the midrib. Fibres connected to the 830 nm LED of the ED800T detector of the PAM 101 chlorophyll fluorometer (H. Walz, Effeltrich, Germany) guide the measuring beam to the leaf cuvette, where it crosses two glass windows and water jacket before entering the leaf. The end of the collecting bundle, leading to the photodiode of the same detector, is placed 3 mm from the lower side of the leaf. By replacing the leaf with white opal glass or white paper it was confirmed that the 830 nm signal is insensitive to superimposed WL. The signal is sampled by a computer datalogger at 50 μs intervals. Several readings are averaged dependent on the time constant of the recorded transient. Several transients could be collected and averaged in order to increase the signal/noise ratio. Data are analysed by means of a program which fits a sum of two exponents with the data points, allowing a drifting baseline if necessary.

Leaf absorbance is measured comparing the backscattered and transmitted photon fluxes from the leaf and from a high-scattering opal glass replica. Measurements are done with the LI-190SB sensor which replaces the 830 nm LED port (for reflection) and photodiode port (for transmission). Light data are presented as the photon absorption density (PAD).

A 1000 W DC Xenon arc lamp, equipped with cold mirror and OCLI heat-reflecting filter (to cut off radiation to which the 830 nm signal detector is sensitive), provides the actinic WL for photosynthesis. Irradiation density is changed by filters and by controlling the lamp current. A spring-operated revolving shutter interrupted the actinic beam within 0.6 ms. Far-red light which predominantly exites PS I is provided by a Schott KL 1500 light source equipped with an interference filter with maximum at 720 nm and half bandwidth 10 nm. The FRL contains about 10% PS II light and does not interfere with the 830 nm measurements.

Results

Heterogeneity of the postillumination kinetics of $P700^+$ reduction in the leaf

Figure 1 shows transients in the 830 nm signal from different PADs to the dark. CO_2 exchange and 830 nm signal were stabilized at each PAD in sequence from higher to lower as shown in Table 1 for data points 1 to 7. At the end of each exposure light was interrupted 10 times for 0.5 s (interval 10 s), and the 830 nm signal transients collected. The quality of the recordings in 1 and 10 repetitions is shown for the curve 1. Measurements were difficult at strictly limiting PADs due to the small signal amplitude.

Slow drifts in the 830 nm signal, not related to P700 oxidation changes (Klughammer and

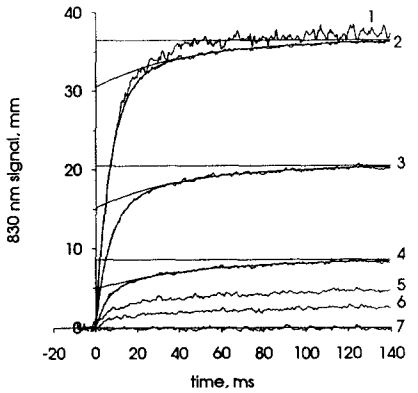

Fig. 1. Postillumination transients in the 830 nm signal from a sunflower leaf (specification of conditions in Table 1, data points 1 to 7). CO_2 exchange and 830 nm signal were stabilized at each PAD in sequence from higher to lower. At the end of each exposure the leaf was darkened 10 times for 0.5 s (interval 10 s), and the transients collected. Initial S830 levels shifted into coincidence. Difference in the quality of the computer recording in 1 and 10 repetitions is shown for the curves 1 and 2. Least-square approximations of curves 2, 3 and 4 with two exponents are shown.

Table 1. Results of the measurements of postillumination $P700^+$ reduction kinetics under different photon absorption densities (PAD), cell-wall CO_2 concentrations (C_w), O_2 concentrations and leaf temperatures (t_l) with a sunflower leaf. $P700^+$ reduction time-constants T_1 and T_2 and their corresponding amplitudes a_1 and a_2 are found from a two-exponent fit as shown in Fig. 1. Data points numbered in sequence of experimental procedures

Point no.	t_l (°C)	O_2 (%)	PAD (nmol $cm^{-2} s^{-1}$)	C_w (μM)	P (nmol $cm^{-2} s^{-1}$)	T_1 (ms)	a_1 (mm)	T_2 (ms)	a_2 (mm)
Exp. 888. Light curve in 21% O_2									
1	22.5	21	134.3	8.58	3.25				
2	22.5	21	134.3	8.59	3.26	6.7	30.0	42	6.0
3	22.1	21	84.4	8.92	3.00	6.5	14.8	41	5.3
4	21.9	21	43.5	10.09	2.15	5.4	4.8	46	3.7
5	21.8	21	26.9	10.97	1.51	6.6	2.5	73	2.3
6	21.7	21	14.5	11.91	0.84	3.5	1.6	102	2.0
7	21.6	21	0.0	13.32	−0.15				
Photosynthetic induction									
8	22.5	21	134.3	11.5	0.99	20	62.1	181	5.6
9	22.5	21	134.3	10.4	1.84	13.4	53.8	–	0.0
10	22.5	21	134.3	9.36	2.66	6.5	24.0	16.2	19.7
CO_2 compensation point and CO_2-free air									
16	22.4	21	134.3	1.53	0.03	9.5	30.6	18.3	27.2
24	22.4	21	134.3	0.54	−0.43	9.9	37.8	24.7	14.8
Light curve in 1.2.% O_2									
33	22.5	1.2	136.2	4.41	3.18	8.9	26.3	21.8	19.1
34	22.1	1.2	84.4	4.66	3.01	8.4	13.9	25.5	15.2
35	21.9	1.2	44.8	5.48	2.39	6.9	6.1	36.7	6.7
36	21.8	1.2	27.7	6.39	1.69	6.3	3.3	50.2	4.2
37	21.7	1.2	14.2	7.41	0.91	6.7	1.2	66.6	2.6
38	21.6	1.2	0.0	8.76	−0.14				

Schreiber 1991), are considered in the analysis of these transients as the drift of the dark base line. From 0 to 140 ms the transients can be approximated with a sum of two exponents, shown for three measurements in Fig. 1. For these and other measurements the experimental conditions and time-constants of $P700^+$ reduction are given in Table 1. The time constant for the fast exponent T_1 is about 6 ms and it depends only slightly on light intensity in this experiment. The time constant for the slower exponent T_2 is about 40 ms and it seems to increase towards lower PADs. The amplitude of the slower exponent makes about 20% of the total change at higher PADs, but its relative role increases at lower PADs. The factors which may contribute to this heterogeneity are

1. the heterogeneity of chloroplasts in the leaf cross-section caused by the adaptation to different average light intensities (Laisk and Oja 1976),
2. heterogeneity of the origin of the 830 nm signal which contains components from P700, PC and Fd (Klughammer and Schreiber 1991) and,
3. the connection of the population of PS I in a thylakoid to heterogenous electron donors.

The tendency that the slower process forms a greater part of the amplitude at low PADs provides evidences contrary to the first possibility since in this case the ratio should be constant. Plastocyanin rapidly donates electron to $P700^+$ (Haehnel 1984) and cannot be a cause for the slow component of $P700^+$ reduction. Thus, it seems that a fraction of PS I population is connected to slower electron donors than the rest of the PS I centres. Assuming that the slower electron donors still participate in the

linear electron transport we can calculate the fraction of the total linear electron transport carried by the slow PS I population f_s as

$$f_S = \frac{a_2/T_2}{a_1/T_1 + a_2/T_2} \quad (1)$$

where a is amplitude, T is time constant and 1 and 2 denote fast and slow components, respectively.

At high rates the slow PS I population carries only about 3% of the total linear electron flow. At low PADs this fraction increases to 8–10%. If the slow fraction participates in the cyclic electron flow then it does not contribute to the linear flow. Since the slow component is, at most, a minor contributor to linear electron flow we shall neglect the slow population of PS I centres and study the variations of the rapid time constant of the postillumination 830 nm transient only. For this reason the two-exponent analysis was not always used but the initial part of the postillumination process was approximated with one exponent.

Light dependence of the postillumination $P700^+$ reduction kinetics

From Fig. 1 and the data in Table 1 one can see that the fast time constant T_1 of the postillumination 830 nm signal only decreases slightly from saturating to limiting PADs. This result coincides with that of Harbinson and Hedley (1989) who obtained similar time-constants for the postillumination $P700^+$ reduction in pea leaves. Clearly, resistance to PQH_2 oxidation rate changes very little over the range of used PADs at 21% O_2 and near-atmospheric CO_2 concentrations. This means that either photosynthethic control of electron flow by proton counterpressure at the site of plastoquinol oxidation is absent under normal air conditions, or it is still present but constant.

Kinetics of postillumination $P700^+$ reduction at limited electron transport rates

Electron transport rates were limited by lowering the CO_2 concentration or employing photosynthetic induction. When CO_2 concentration was lowered to the compensation point at 21% O_2, and further to 0, T_1 increased (Table 1), as well as the amplitude of the slower exponent. Photosynthetic control was maximum during the induction of photosynthesis after a dark exposure, when T_1 increased to 20 ms in the beginning of the induction and then gradually decreased to 6.5 ms. When the light dependence was measured under the same ambient CO_2 concentration but at 1.2% O_2, T_1 was equal to that in 21% O_2 at limiting PADs, but significantly increased at light saturation.

The ETR was further limited by lowering the CO_2 concentration at low O_2 (Table 2). In the first experiment at 1.2% O_2 the time constant is 10.2 ms at the highest CO_2 concentration (which shows the presence of photosynthetic control compared with the data from Table 1) and it increases to 37 ms with decreasing C_w. In the second experiment with the same leaf O_2 evolution rate was measured with the Zirconium-oxide electrode. At 0.005% O_2 the maximum capacity of the photosynthetic control seems to be weaker than in 1.2% O_2, since the maximum T_1 value is about 31 ms compared with 37 ms in 1.2% O_2. During the exposure of the leaf in O_2-free atmosphere at high light intensity the FRL-induced 830 nm signal deflection considerably decreased (Table 2). This shows that under anaerobic conditions at high light intensities a relatively stable population of PS I is formed in which P700 cannot be oxidised by FRL, probably because these PS I centres are incapable of electron transport (Bottin and Sètif 1991). Inhibition of photosynthesis under anaerobic conditions (Ziem-Hanck and Heber 1980) may be related to this phenomenon. This closed state of PS I centres is reversible in the presence of 21% O_2 within 100 s.

Temperature dependence of the $P700^+$ reduction rate

Since temperature influences the photosynthetic rate, we studied its effect on the $P700^+$ reduction kinetics. At PAD 140 nmol cm^{-2} s^{-1} and external CO_2 concentration of 2000 and 330 ppm, leaf temperature was lowered from 22 to 16 and 12 °C (Table 2).

As expected, the rate of postillumination

Table 2. Results of the measurements of CO_2 uptake, O_2 evolution and postillumination $P700^+$ reduction kinetics under different CO_2 concentrations at 1.2% and 0.005% O_2 in ambient gas and at different leaf temperatures. The postillumination $P700^+$ reduction kinetics approximated by one exponent over the span of 4 time-constants T_1. Data points numbered in sequence of experimental procedures. $D830_{frl}$ denotes the deflection of the 830 nm signal from the dark level under FRL (given for 3 data lines)

Point no.	t_l (°C)	O_2 (%)	PAD (nmol $cm^{-2} s^{-1}$)	C_w (μM)	P (nmol $cm^{-2} s^{-1}$)	T_1 (ms)	$D830_{fr}$ (mm)
Exp. 881: CO_2 curve at 1.2% O_2							
6	22.7	1.2	81.2	5.31	1.78	16.2	
7	22.7	1.2	81.2	3.17	1.11	20.3	
8	22.7	1.2	81.2	2.16	0.72	24.5	
9	22.7	1.2	81.2	1.60	0.52	28.9	
10	22.7	1.2	81.2	0.79	0.29	37.4	
11	22.7	1.2	132.1	9.92	1.81	10.2	
Exp. 882: CO_2 curve of O_2 evolution at 0.005% O_2							
1	22.7	0.005	132.1	–	2.96	12.0	
2	22.7	0.005	132.1	–	1.15	17.5	58
3	22.7	0.005	132.1	–	2.23	13.0	
4	22.7	0.005	132.1	–	0.67	20.1	
5	22.7	0.005	132.1	–	0.59	24.0	33
6	22.7	0.005	132.1	–	0.33	27.3	
7	22.7	0.005	132.1	–	0.30	30.7	18
Exp. 880: Temperature dependence at saturating CO_2							
21	22.4	21	140.7	40.3	3.13	12.0	
12	16.2	21	140.7	50.3	2.11	16.8	
15	12.2	21	140.7	58.9	1.24	21.9	
Temperature dependence at atmospheric CO_2							
13	22.3	21	140.7	10.07	2.28	10.2	
9	16.4	21	140.7	12.54	1.92	13.2	
14	12.2	21	140.7	15.31	1.43	19.7	

$P700^+$ reduction decreases at lower temperatures, as does the photosynthetic rate. This may be the direct effect of temperature on the rate-constant of PQH_2 oxidation and not necessarily related to the photosynthetic control, but if the most temperature-sensitive reaction is downstream of PS I, the slower oxidation of PQH_2 at lower temperatures may be induced by the photosynthetic control.

$P700^+$ reduction kinetics in the course of photosynthetic oscillations

After a rapid transition from limiting to saturating CO_2 the new steady-state photosynthetic rate becomes established after a deep transient minimum and a series of oscillations. The minima of oscillations are accompanied by reduction of P700 which is caused by accumulation of electrons at the acceptor side of PS I (Laisk and Oja 1991, Laisk et al. 1991, Laisk et al. 1992c). In order to study the kinetics of $P700^+$ reduction, repeated transients from 300 to 2000 ppm CO_2 were interrupted at different phases of oscillations by sudden darkening and one transient of 830 nm signal was recorded. A phase-portrait where the quantum yield of electron transport (calculated as 4 times gross photosynthetic rate divided by PAD) is plotted against the D830 signal (difference from the dark level) is shown in Fig. 2. The process begins at a high electron transport rate (quantum yield $Y = 0.2$) when the $P700^+$ reduction is rapid ($T_1 = 7.5$ ms). The trough in photosynthesis is accompanied by a significant PS I acceptor side reduction which is indicated by the movement of the phase trajectory down and to the left. No intensification of the donor side control occurs during this phase since T_1 stays constant at 8 ms. The photosynthetic control of electron flow at the PS I

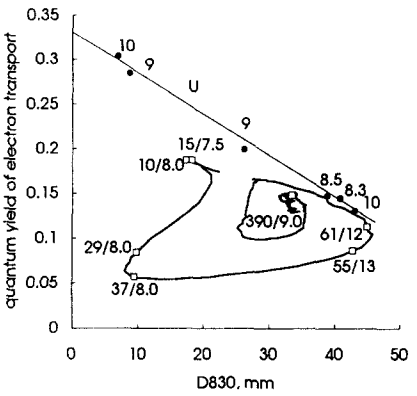

Fig. 2. Phase-portrait of the quantum yield of electron transport versus D830 signal (difference from the dark level). Oscillations were initiated by a transition from 300 to 2000 ppm CO_2. The transition was repeated, interrupted at different phases of oscillations by sudden darkening, and the 830 nm signal recorded. The quantum yield of electron transport $Y = 4 \cdot$(gross photosynthetic CO_2 uptake rate)/PAD is plotted against the D830 signal with 2 s intervals. Current time (s) from the moment of transition and the corresponding postillumination $P700^+$ reduction time constants are shown at different phases of the oscillation. Steady-state points measured with the same leaf at different PADs are joined with a straight line U and the corresponding $P700^+$ reduction time-constants are shown at data points. Recording of the phase trajectory was stopped at t = 390 s, before it approached steady-state after 15 min (see also Laisk and Oja 1991, Laisk et al. 1992c).

donor side increases after the minimum in the photosynthetic rate and maximum acceptor side reduction, since in the next measurement (20 s after the minimum) $T_1 = 13$ ms. Photosynthetic control decreases again when the oscillation trajectory approaches the steady-state points where the acceptor side reduction is in minimum. After oscillations (390 s) the phase trajectory stays to the left from the steady-state line showing small reduction of the PS I acceptor side, but this slowly disappears and the trajectory finally approaches the steady-state line. On the basis of the deflection of the phase portrait data points from the donor-side limited steady-state points we concluded that during oscillations rate-limiting control is swinging from the PS I donor side to the acceptor side and back (Laisk et al. 1992c). The above measurements of $P700^+$ reduction kinetics confirm this conclusion. Additionally, these measurements show a delay in the onset of the photosynthetic control until the photosynthetic rate drops to the minimum.

Time-kinetics of the photosynthetic control

A sudden limitation of electron transport rate, e.g. by lowering CO_2 concentration, causes temporary accumulation of electrons on the acceptor and donor sides of PS I. These sites become oxidised again after the down-regulation of the PQH_2 oxidation rate. Figure 3 shows transients in the 830 nm signal after decreasing CO_2 concentration. At first the 830 nm signal increases rapidly showing reduction of $P700^+$. Temporarily the signal even exceeds the dark level which, probably, reflects transient reduction of ferredoxin (Klughammer and Schreiber 1991). The time for reoxidising P700 is longer the lower the final CO_2 concentration, and, thus, the electron transport rate, extending from 15 to 40 s. Reduction of the PS I acceptor side becomes permanent, unoxidisable by FRL in the absence of O_2 (Table 2). We suggest that similar type kinetics of photosynthetic control causes the delay which leads to oscillations in photosynthesis (Laisk and Eichelmann 1989).

Cyclic electron flow or acceptor side reduction of PS I complexes?

Considering that the rate of electron flow during the postillumination transient is determined by

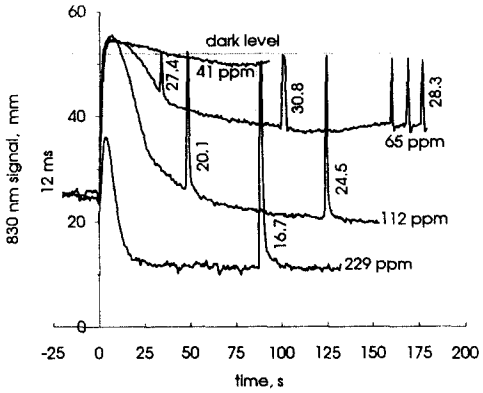

Fig. 3. Transients in the 830 nm signal after CO_2 concentration was decreased from 462 ppm to different lower levels, shown at the ends of the curves. Other conditions see Table 2, $O_2 = 0.005\%$). Light–dark transitions to measure the $P700^+$ reduction kinetics are seen in the recordings (corresponding time-constants T_1 in ms are shown at each transient). T_1 before the transitions to lower CO_2 concentrations was 12 ms.

plastoquinol oxidation at Cyt b_6f, the following relationship holds true:

$$T_p = T_c \cdot N_p/N_c \quad (2)$$

where T_p is the measured time constant for $P700^+$ reduction, T_c is the turnover-time of one Cyt b_6f complex, and N_p and N_c are the concentrations of PS I and Cyt b_6f complexes, respectively. It has been shown that PC forms tight complexes with PS I and Cyt f, so that the stoichiometry of active Cyt b_6f, PC and PS I is 1:2:1 (Haehnel et al. 1980, Haehnel 1982, Graan and Ort 1984). In photosynthetic bacteria one or two Cyt c seem to form a supercomplex with the photoreaction centre (Lavergne and Joliot 1991). On the basis of the $P700^+$ postillumination reduction kinetics in the presence of different concentrations of DBMIB Haehnel (1982) concluded that crossdiffusion of PC between the electron transport chains is possible. On the other hand, on the basis of the proportional decline in the photosynthetic rate with developing PS I acceptor side reduction, an electron-channelling supercomplex between Cyt b_6f, PC, PS I, Fd and FNR has been proposed (Laisk et al. 1992b, Laisk et al. 1992c, Laisk 1993). In this supercomplex crossdiffusion between the electron channels is relatively restricted. On the basis of this model $N_p = N_c$ which makes it possible to find the concentration of PS I centres from measured electron transport rates and time constants of $P700^+$ reduction.

Neglecting the contribution of the slower centres, the electron transport rate ETR can be calculated as

$$ETR = N_p/T_1 \quad (3)$$

where N_p is the number of Cyt b_6f–PC–PS I complexes. In Fig. 4, ETR is plotted against the rate-constant for $P700^+$ reduction $k_1 = 1/T_1$ for the experiments in Tables 1 and 2 plus some additional data. At 1.2% and 0.005% O_2 and at saturating CO_2 concentration in 21% O_2 ETR is calculated as 4 times gross photosynthetic rate. Data points measured at ETR limited by low CO_2 or temperature display significant linear correlation between ETR and $1/T_1$. The points which stay considerably to the right of the dotted regression line are measured at limiting PADs. This shows that at saturating PADs electron transport rate is determined by the rate-constant $1/T_1$ of plastoquinol oxidation which can vary in a range from about 150 to 30 s^{-1}. According to Eq. (3), the slope of the line drawn from the origin of the coordinates to any data point represents the number of PS I centres N_p which are active electron acceptors. At limiting PADs this number of electron transport chains (which have at least one electron vacancy between the sites of PQH_2 oxidation and P700 reduction since only these can be electron acceptors) is smaller because PS I excitation rate does not considerably exceed the electron donation rate from PQH_2. By increasing PAD we arrive at a state where at least one electron vacancy is in all chains. In this case the slope of the solid line in Fig. 4 approaches the maximum value, equal to the number of PS I centres in the leaf sample.

Unexpectedly, the regression in Fig. 4 does not extrapolate to the origin but crosses the axis of ETR below zero and the axis of $1/T_1$ above zero. These facts suggest two interpretations. First, an electron flow undetectable by our techniques may be present. This can rather be cyclic electron flow than nitrite reduction since the latter would have been detected in the experiment where O_2 evolution was recorded.

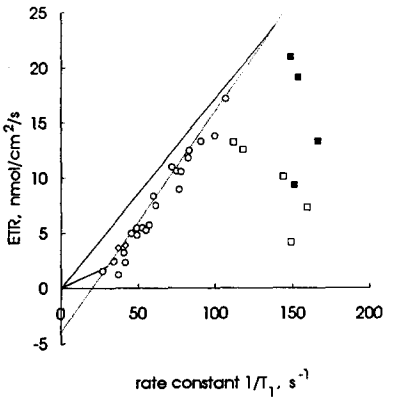

Fig. 4. Electron transport rate ETR, plotted against the rate-constant for $P700^+$ reduction $k_1 = 1/T_1$ from experiments in Tables 1 and 2, plus additional data. Dotted line, linear regression of the data measured at CO_2 and temperature limited electron transport rates. Empty squares correspond to the light curve measured at 1.2% O_2 (Exp. 888, Table 1). Filled squares correspond to the light curve measured at 21% O_2 in the same experiment (ETR calculated from Eq. (4)).

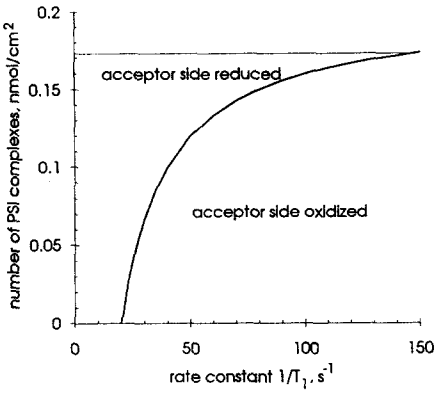

Fig. 5. Dependence between the rate-constant for plastoquinol oxidation $1/T_1$ and the fractions of the PS I centres with reduced and oxidised acceptor sides, calculated from Fig. 4. as the slope of the line drawn from the origin of coordinates to different points of the dashed line.

However, it is difficult to conceive how this flow can be constant at different CO_2 limitations and different temperatures. Furthermore, at strictly CO_2-limited rates the plastoquinone pool is likely to be highly reduced, preventing cyclic flow through plastoquinone due to the absence of the necessary redox poising (Arnon and Chain 1977).

Another interpretation assumes that our regression line is only apparently linear, i.e., each data point has its own N_p, as shown by the two solid lines as examples. In this case the maximum N_p occurs at the top of the area covered by data points and equals to 0.15 nmol cm^{-2} of PS I centres for the highest data point. When electron transport becomes gradually more limited downstream PS I by low CO_2 or temperature, gradually fewer PS I centres can be active electron acceptors, probably because of their closure by acceptor side reduction. The calculated number of actively operating Cyt b_6f complexes drops to 0.067 nmol cm^{-2} at strictly limited electron transport rates. According to this result, PS I acceptor side reduction increases in parallel with stronger photosynthetic control of PQH_2 oxidation rate (Fig. 5).

Discussion

The time-constants of the postillumination $P700^+$ reduction obtained in this work on sunflower leaves agree well with those obtained by Harbinson and Hedley (1989) on pea leaves. The $t_{1/2}$ of 4.5 ms in that work corresponds to T_1 of 6.5 ms which coincides with the T_1 for the light curves in Table 1. Other reported $t_{1/2}$ values are also comparable with our result: 4–5 ms (Maxwell and Biggins 1977); 6 ms (Siggel 1974); 5 ms for cytochrome reduction (Crowther and Hind 1980). It shows that the minimum time constant for PQH_2 oxidation is rather similar in different plant species. This good coincidence of different data supports the notion that T_1 is a fundamental parameter of the photosynthetic machinery, the turnover rate of the limiting step in a unit of electron transport chain (Haehnel 1982). The good agreement of the $P700^+$ dark reduction time-constants obtained in our work with the results of other investigators supports the reliability of the 830 nm signal as an indicator of the P700 oxidation state in leaves.

The maximum number of electron transport chains obtained from data points in Fig. 4 is $N_p = 0.15$ nmol cm^{-2}. Based on the chlorophyll content in sunflower leaves of about 50 μg cm^{-2} we calculate a ratio of 1 P700 per 370 Chl. This is somewhat greater than reported (Graan and Ort 1984, Glazer and Melis 1987), but one has to consider that sunflower leaves have much higher photosynthetic rates than spinach and, probably, contain more electron carriers. In our sunflower leaves the maximum rate of electron transport supported by all Cyt b_6f–PS I complexes would be 0.15 nmol $cm^{-2}/0.006$ s = 25 nmol cm^{-2} s^{-1} or 25/4 = 6.25 nmol cm^{-2} s^{-1} of O_2 evolution. In the phase of the photosynthetic induction where ETR was limited by PQH_2 oxidation the O_2 evolution rate was about 6 nmol cm^{-2} s^{-1} in similarly grown sunflower leaves (Kiirats 1985, Laisk et al. 1992a).

The major problem which has not allowed us to mathematically reproduce oscillations in photosynthesis has been the lack of enough delay in feedback loops (Laisk and Eichelmann 1989). This work shows that the delay must be sought in the processes which occur during the highly reduced phase of oscillations and which lead to the reestablishment of the control of electron transport at the site of plastoquinol oxidation. Correlation between the reduction level of the PS I acceptor side and the photosynthetic control

(Figs. 4 and 5) may be causal. Hind and coworkers (1981) suggested that the redox state of electron carriers around PS I may control reallocation of electron flow from linear to cyclic and, thus, induce photosynthetic control through the increasing luminal proton concentration.

This work shows that the usable range of photosynthetic control is between $1/T_1 = 160$ and 40 to 50 s^{-1}, i.e. about 3 to 4 times. It is interesting to see which stress conditions such range satisfies. Under atmospheric conditions, in the presence of 21% O_2 the ETR can be calculated using a derivation from the model (Farquhar and von Caemmerer 1982)

$$ETR = \frac{4 \cdot P \cdot (K_{sp} + [O_2]/[CO_2])}{K_{sp} - 0.5[O_2]/[CO_2]} \quad (4)$$

where P is net CO_2 photoassimilation rate (gross photosynthesis minus photorespiration) and K_{sp} is the specificity factor of rubisco. Big filled squares in Fig. 4 are calculated from Eq. (4) on the basis of the light curve measured under 21% O_2 in Table 1 taking $[O_2] = 254\ \mu M$, $[CO_2] = C_w$ and $K_{sp} = 97$ (Laisk 1977). One can see that in air there are enough acceptors to support electron flow as rapid as the basic reaction rate of the Cyt b_6f complexes and their abundance allow. Very little photosynthetic control is needed (slight declination of the data points to the left at higher rates). Such a free electron transport is possible due to cooperation of photosynthesis and photorespiration. At the CO_2 compensation point (e.g., closed stomata) the measured $T_1 = 9.5$ ms (Table 1) which corresponds to internal electron transport rate about 13 nmol cm^{-2} s^{-1} (Fig. 4, at $1/T_1 = 105\ s^{-1}$). As we see, at this electron transport rate photosynthetic control is easily possible and not much PS I acceptor side reduction appears. Doubling the rubisco specificity for CO_2 would decrease the internal electron transport at the CO_2 compensation to 6.5 nmol cm^{-2} s^{-1} which would require holding the PQH_2 oxidation rate-constant at 60 s^{-1}. About 35% of the PS I complexes have reduced acceptor sides when photosynthetic control is so strong (Fig. 5). Thus, reduction of photorespiration in C_3 plants would lead to higher reduction of electron transport chains when stomata are closed and it must be studied how much long-lasting reduction is allowed without danger of damage.

The fact that under normal physiological conditions leaves function at the maximum capacity of their PQH_2 oxidation system and the latter is suppressed only under stress conditions needs to be paralleled with in vitro studies of proton translocation and photophosphorylation. Channelled proton transport from Cyt b_6f to the CF_o coupling factor proceeds without equilibration of protons with the thylakoid lumen when phosphorylation conditions are favourable and the thermodynamic proton pressure is not high enough to destroy the Ca^{+2} bridges isolating the intramembranal proton conducting channels from the lumen (Chiang and Dilley 1989, Laasch et al. 1993). Under these conditions the lumen does not acidify much, though ATP synthesis is going at full speed. To the contrary, when phosphorylation is restricted (low ADP or Pi), the increasing intramembranal proton pressure leads to the dissociation of the Ca^{+2} bridges and protons are released into the lumen. It is generally accepted that the rate of PQH_2 oxidation is controlled by the luminal pH. This explains the absence of photosynthetic control under conditions favourable for phosphorylation and the presence of this control under conditions where photophosphorylation is restricted. From this viewpoint, luminal acidification has a regulatory function, and may not even be obligatory for photophosphorylation in vivo (Ohmori et al. 1985).

Acknowledgement

This work was supported by Volkswagenstiftung grant I/67762. Discussion with and help from Dr R. Peterson (The Connecticut Agricultural Experiment Station) is appreciated.

References

Arnon DI and Chain RK (1977) Role of oxygen in ferredoxin-catalyzed cyclic photophosphorylations. FEBS Lett 82(2): 297–302

Bendall DS (1982) Photosynthetic cytochromes of oxygenic organisms. Biochim Biophys Acta 683: 119–157

Bottin H and Sètif P (1991) Inhibition of electron transfer

from A_0 to A_1 in Photosystem I after treatment in darkness at low redox potential. Biochim Biophys Acta 1057: 331–336

Chiang GG and Dilley RA (1989) Calcium regulation of localized to delocalized proton gradient switching in thylakoids: 8 kDa CF_0 subunit is part of the Ca^{+2} gating structure. In: Strömgren and Allen N (eds) Plant Biology, Photosynthesis, Vol 8, pp 437–455. Alan R. Liss, Inc, New York

Crowther D and Hind G (1980) Partial characterization of cyclic electron transport in intact chloroplasts. Arc Biochem Biophys 204: 568–577

Farquhar GD and von Caemmerer S (1982) Modelling of photosynthetic response to environmental conditions. In: Lange OL, Nobel PS, Osmond CB and Ziegler H (eds) Physiological Plant Ecology. Encycl Plant Physiol, New Series, Vol 12B, pp 549–588. Springer-Verlag, Berlin

Foyer C, Furbank R, Harbinson J and Horton P (1990) The mechanisms contributing to photosynthetic control of electron transport by carbon assimilation in leaves. Photosynth Res 25: 83–100

Genty B, Harbinson J and Baker N (1990) Relative quantum efficiencies of the two photosystems of leaves in photorespiratory and non-photorespiratory conditions. Plant Physiol Biochem 28: 1–10

Glazer AN and Melis A (1987) Photochemical reaction centres: Structure, organization and function. Annu Rev Plant Physiol 38: 11–45

Graan T and Ort DR (1984) Quantitation of the rapid electron donors to P700, the functional plastoquinone pool, and the ratio of the photosystems in spinach chloroplasts. J Biol Chem 259: 14003–14010

Haehnel W (1982) On the functional organization of electron transport from plastoquinone to Photosystem I. Biochim Biophys Acta 682: 245–257

Haehnel W (1984) Photosynthetic electron tyransport in higher plants. Annu Rev Plant Physiol 35: 659–693

Haehnel W, Pröpper A and Krause H (1980) Evidence for complexed plastocyanin as the immediate electron donor of P-700. Biochim Biophys Acta 593: 384–399

Harbinson J and Hedley CL (1989) The kinetics of $P\text{-}700^+$ reduction in leaves: A novel in situ probe of thylakoid functioning. Plant Cell Environ 12: 357–369

Harbinson J and Woodward FI (1987) The use of light-induced absorbance changes at 820 nm to monitor the oxidation state of P-700 in leaves. Plant Cell Environ 10: 131–140

Harbinson J, Genty B and Baker NR (1989) Relationship between the quantum efficiencies of Photosystem I and II in pea leaves. Plant Physiol 94: 545–553

Harbinson J, Genty B and Foyer CH (1990) Relationship between photosynthetic electron transport and stromal enzyme activity in pea leaves. Toward an understanding of the nature of the photosynthetic control. Plant Physiol 94: 545–553

Hind G, Crowther D, Shahak Y and Slovacek RE (1981) The function and mechanism of cyclic electron transport. In: Akoyunoglou G (ed) Photosynthesis II. Electron Transport and Photophosphorylation, pp 87–97. Balaban International Science Services, Philadelphia, PA

Joliot P and Joliot A (1984) Electron transfer between the two photosystems. II. Equilibrium constants. Biochim Biophys Acta 765: 219–226

Kiirats O (1985) Kinetics of CO_2 and O_2 exchange in sunflower leaves during the light–dark transition. In: Viil J, Grishina G and Laisk A (eds) Kinetics of Photosynthetic Carbon Metabolism in C_3 Plants, pp 131–135. Valgus, Tallinn

Klughammer C and Schreiber U (1991) Analysis of light-induced absorbance changes in the near-infrared spectral region. I. Characterization of various components in isolated chloroplasts. Z Naturforsch 46c: 233–244

Laasch H, Ihle C and Gunther G (1993) Detecting localized proton currents in photophosphorylation by procaine inhibition of the transthylakoid pH-gradient. Biochim Biophys Acta 1140: 251–261

Laisk A (1977) Kinetics of Photosynthesis and Photorespiration in C_3 Plants. Nauka, Moscow, 198 pp

Laisk A (1993) Mathematical modelling of free-pool and channelled electron transport in photosynthesis: Evidence for functional supercomplex around Photosystem I. Proc R Soc Ser B 251: 243–251

Laisk A and Oja V (1976) Adaptation of the photosynthetic apparatus to light profile in the leaf. Fiziologija Rastenij (Sov Plant Physiol) 23(3): 445–451 (in Russian)

Laisk A and Eichelmann H (1989) Towards understanding oscillations: A mathematical model of the biochemistry of photosynthesis. Phil Trans R Soc Lond 323: 369–384

Laisk A and Oja V (1991) The response of leaf photosynthesis to elevated CO_2. In: Abrol YP, Govindjee, Wattal PN, Ort DR, Gnanam A and Teramura AH (eds) Impact of Global Climatic Changes on Photosynthesis and Plant Productivity, pp 233–264. Oxford and IBH, New Delhi Bombay Calcutta

Laisk A, Siebke K, Gerst U, Eichelmann H, Oja V and Heber U (1991) Oscillations in photosynthesis are initiated and supported by imbalances in the supply of ATP and NADPH to the Calvin cycle. Planta 185: 554–562

Laisk A, Kiirats O, Oja V, Gerst U, Weis E and Heber U (1992a) Analysis of oxygen evolution during photosynthetic induction and in multiple-turnover flashes in sunflower leaves. Planta 186: 434–441

Laisk A, Oja V and Heber U (1992b) Steady-state and induction kinetics of photosynthetic electron transport related to donor side oxidation and acceptor side reduction of Photosystem I in sunflower leaves. Photosynthetica 27: 449–463

Laisk A, Oja V, Walker D and Heber U (1992c) Oscillations in photosynthesis and reduction of Photosystem I acceptor side in sunflower leaves. Functional Cyt *b/f*–PS I–FNR complexes. Photosynthetica 27: 465–479

Lavergne J and Joliot P (1991) Restricted diffusion in photosynthetic membranes. TIBS 16: 129–134

Lechtenberg D, Voss B and Weis E (1990) Regulation of photosynthesis: Photosynthetic control and thioredoxin-dependent enzyme regulation. In: Baltscheffsky M (ed) Current Research in Photosynthesis, Vol IV, pp 171–174. Kluwer Academic Publishers, Dordrecht

Maxwell PC and Biggins J (1977) The kinetic behaviour of P-700 during the induction of photosynthesis in algae. Biochim Biophys Acta 459: 442–450

Ohmori M, Gimmler H, Schreiber U and Heber U (1985)

Relative insensitivity of photosynthesis to the dissipation of a transthylakoid proton gradient in intact chloroplasts. Physiol Veg 23(5): 801–812

Oja VM (1983) A rapid-response gas exchange measuring device for studying the kinetics of leaf photosynthesis. Fiziologija Rastenij (Sov Plant Physiol) 30: 1045–1052

Rich P (1982) A physicochemical model of quinone-cytochrome *b–c* complex electron transfers. In: Trumpower BL (ed) Functions of Quinones in Energy Consuming Systems, pp 73–83. Academic Press, New York

Schreiber U, Klughammer C and Neubauer C (1988) Measuring P700 absorbance changes around 830 nm with a new type pulse modulation system. Z Naturforsch 43c: 686–698

Siggel U (1974) The control of electron transport by two pH-sensitive sites. In: Avron M (ed) Proc 3rd Int Congress Photosynthesis, pp 645–654. Elsevier, Amsterdam

Siggel U (1976) The function of plastoquinone as an electron and proton carrier in photosynthesis. Bioelectrochemistry and Bioenergetics 3: 302–318

Stiehl HH and Witt HT (1969) Quantitative treatment of the function of plastoquinone in photosynthesis. Z Naturforsch 246: 1588–1598

Weis E and Lechtenberg D (1989) Fluorescence analysis during steady-state photosynthesis. Phil Trans R Soc Lond B 323: 253–268

Weis E, Ball JT and Berry JA (1987) Photosynthetic control of electron transport in leaves of *Phaseolus vulgaris*. In: Biggins J (ed) Proc 7th Int Congress Photosynthesis, Vol 2, pp 553–556. Martinus Nijhoff, Dordrecht

Ziem-Hanck U and Heber U (1980) Oxygen requirement of photosynthetic CO_2 assimilation. Biochim Biophys Acta 591: 266–274